

Structural and optical properties of photocrystallized Se films

Takeshi Innami and Sadao Adachi

Department of Electronic Engineering, Faculty of Engineering, Gunma University, Kiryu-shi, Gunma 376-8515, Japan

(Received 2 April 1999)

Structural and optical properties of photocrystallized Se films have been studied using x-ray diffraction (XRD), spectroscopic ellipsometry (SE), and *ex situ* atomic force microscopy (AFM) techniques. The amorphous (*a*-) Se films used are deposited by vacuum evaporation on glass substrates at 300 K. Photocrystallization is performed using a linearly polarized 488.0-nm line of an Ar laser. For comparison, thermocrystallized films at 100 °C for 1 h in a dry N₂ atmosphere are studied. The XRD pattern shows that the photocrystallized film is characterized by a polycrystalline structure with which the (10 $\bar{1}$ 0) plane is preferentially grown. The SE data also give that the *c* axis is perpendicular to the direction of the polarization of the illuminating light. The thermocrystallized film, on the other hand, shows an unoriented polycrystalline nature. The dielectric functions for these two films are considerably smaller than those for a bulk, single-crystalline Se. This is mainly due to the roughened surfaces of the photo- and thermocrystallized films. The change in surface morphology after photo- and thermocrystallization is independently assessed by the AFM. [S0163-1829(99)05535-6]

I. INTRODUCTION

Amorphous (*a*-) chalcogenide semiconductors are known to exhibit various photoinduced phenomena, such as photocrystallization,¹ photoinduced anisotropy,² and photodarkening,³ promising that they can be used as materials for optical memory devices. *a*-Se is the simplest representative of amorphous chalcogenide semiconductors. Photocrystallization was first observed by Dresner and Stringfellow.¹ They found that the highly absorbed 200-W Hg arc light enhances the crystallization rate of *a*-Se into hexagonal crystals as much as an order of magnitude. Now, it is known as a common property of chalcogenide glasses when excited with either interband- or subgap-polarized and even unpolarized light.

Photostructural change in *a*-Se has been studied by x-ray diffraction (XRD),^{4,5} *in situ* extended x-ray absorption fine structure,^{6,7} and Raman scattering measurements.^{5,7,8} It has also been reported on a polarized-light-induced anisotropy in the refractive index^{4,9} and optical absorption^{10,11} of *a*-Se films. These studies give a deep understanding of the photocrystallized Se properties. However, its mechanism is still under discussion.

Spectroscopic ellipsometry (SE) is an advantageous technique to measure the optical response of solids. This technique is unquestionably more powerful than conventional reflectometry technique for a number of reasons.¹² For example, it can directly determine the complex dielectric constant, $\varepsilon(E) = \varepsilon_1(E) + i\varepsilon_2(E)$, on a wavelength-by-wavelength basis without having to resort to multiple measurements or to Kramers-Kronig analysis. To our knowledge, however, no SE study has been performed on photo- or thermocrystallized Se films to date. No or little data are also available on the optical constants of such materials at high photon energies. Knowledge of the optical constants of semiconductors is of great importance in the design and analysis of various optical devices using these semiconductors.

In this paper we report on structural and optical properties of the photocrystallized Se films studied using XRD, SE, and

ex situ atomic force microscopy (AFM) measurement techniques. For comparison, thermocrystallized films at 100 °C for 1 h in a dry N₂ atmosphere are investigated.

II. EXPERIMENTAL

The *a*-Se films were deposited by vacuum evaporation in a base pressure of 2×10^{-6} Torr on Corning 7059 glasses at room temperature. The purity of the Se source was 99.9999% (6N). The deposited film thickness was measured to be about 0.85 μm using a Talystep profilometer.

Photocrystallization was performed by illuminating with a linearly polarized 488.0-nm line of an Ar laser at room temperature. The laser-power density of ~ 20 W/cm² used in this study allows us to heat the sample nearly equal to the temperature of *a*-Se softening ($T_g \sim 30$ °C, glass transition temperature).^{8,13} In order to obtain a large photocrystallized area, a light spot in 0.7-mm-diameter was scanned over the sample surface (~ 50 mm²) at a rate of ~ 1.3 mm²/h. For comparison, thermocrystallization was carried out by annealing the *a*-Se samples at 100 °C for 1 h in a dry N₂ atmosphere.

The crystalline quality of the photo- and thermocrystallized films was evaluated by the XRD (RAD-IIC, Rigaku Co., Ltd.) with Cu *K* α radiation. The diffraction traces were obtained at the $\theta-2\theta$ scanning mode.

The SE instrument used in this study was of a rotating analyzer type (DVA-36VW-A, Mizojiri Optical, Co., Ltd.). A 150-W xenon lamp was used as the light source. The SE measurements were performed at room temperature in air over the photon-energy range of 1.2–5.2 eV. The angle of incidence was set at 70° with a polarization azimuth of 45°.

Surface morphology of the photo- and thermocrystallized Se films was investigated by means of an *ex situ* AFM, using a Digital Instruments Nanoscope III. The AFM images were acquired in the tapping mode and in the repulsive force regime with a force constant of the order of 1 nN between the AFM tip and sample surface.

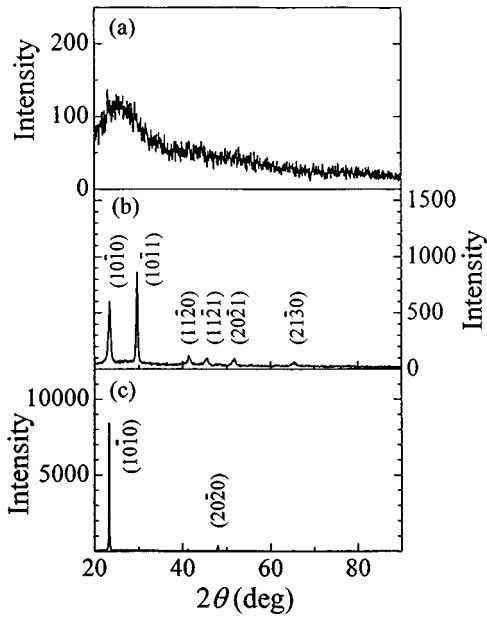


FIG. 1. XRD traces for (a) the as-deposited a -Se, (b) thermocrystallized (100 °C, 1 h), and (c) photocrystallized Se films.

III. RESULTS

A. XRD measurements

Figure 1 shows the XRD traces measured by using the $\theta-2\theta$ scan mode for (a) the as-deposited a -Se, (b) thermocrystallized, and (c) photocrystallized Se films. We can see that for the as-deposited a -Se film [Fig. 1(a)] only a diffuse peak is observed at $2\theta \sim 23.4^\circ$. The fact indicates that the structure of the as-deposited film is surely amorphous.

The thermocrystallized film in Fig. 1(b) shows some relatively strong peaks at $2\theta \sim 23.5^\circ$, $\sim 29.7^\circ$, $\sim 41.9^\circ$, $\sim 44.9^\circ$, $\sim 51.9^\circ$, and $\sim 65.2^\circ$. These peaks can be indexed from an ASTM card of the hexagonal Se as $(10\bar{1}0)$, $(10\bar{1}1)$, $(11\bar{2}0)$, $(11\bar{2}1)$, $(20\bar{2}1)$, and $(21\bar{3}0)$, respectively. We can, thus, rightly conclude that the structure of the thermocrystallized film is polycrystalline. The full width at the half maximum (FWHM) of the two main peaks are, respectively, $\sim 2.4^\circ$ [$(10\bar{1}0)$] and $\sim 1.4^\circ$ [$(10\bar{1}1)$].

The XRD trace of the photocrystallized film [Fig. 1(c)], on the other hand, reveals a very strong peak at $2\theta \sim 23.4^\circ$ [$(10\bar{1}0)$] and its second weak peak at $2\theta \sim 48.0^\circ$ [$(20\bar{2}0)$]. This implies a preferred surface orientation of the photocrystallized film, i.e., the crystallites with the $(10\bar{1}0)$ plane parallel to the substrate surface are predominate. The $(10\bar{1}0)$ -peak FWHM value $\sim 0.9^\circ$ for the photocrystallized film is also found to be considerably smaller than that for the thermocrystallized value ($\sim 2.4^\circ$), suggesting higher crystalline quality of the former film.

B. $\varepsilon(E)$ measurements

We have measured the $\varepsilon(E)$ spectra for the thermo- and photocrystallized Se films by SE in the 1.2–5.2-eV photon-energy range at room temperature. Since hexagonal (or trigonal) material is optically anisotropic, the films have been first of all measured at various configurations, i.e., by rotating the

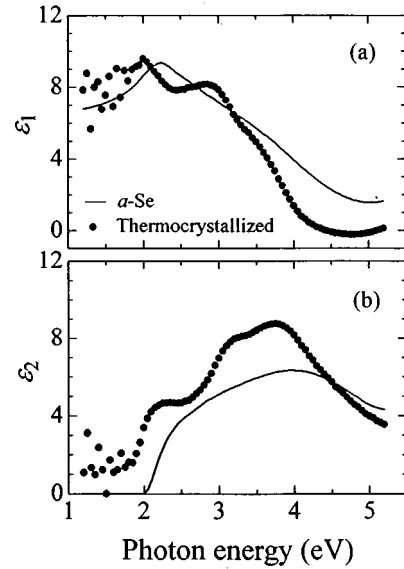


FIG. 2. $\varepsilon(E)$ spectra for the thermocrystallized film (100 °C, 1 h), together with those for the as-deposited a -Se film (Ref. 14).

specimen around the axis perpendicular to their surface and also by varying the angle of incidence and polarizer azimuth. The measured $\varepsilon(E)$ spectra showed no clear difference against specimen rotation for the thermocrystallized film and a remarkable difference for the photocrystallized one, respectively.

1. Thermocrystallized film

The fact that no clear difference in the $\varepsilon(E)$ spectra against specimen rotation for the thermocrystallized film strongly suggests a random orientation of the crystallites in the film. This is in agreement with the XRD result (i.e., an unoriented polycrystalline film). Figure 2 shows the $\varepsilon(E)$ spectra for the thermocrystallized film, together with those for the as-deposited a -Se film (Ref. 14). The oscillations seen in the low photon-energy region ($E < 2$ eV) originate from multiple internal reflections in the evaporated film where it is effectively transparent.

The dielectric function $\varepsilon(E)$ of a crystalline (c -) semiconductor is closely related to its energy band structure, and conclusions about the electronic energy bands can be drawn from features called critical points (CP's) in the $\varepsilon(E)$ spectra.¹⁵ A structureless feature in the $\varepsilon(E)$ spectra of

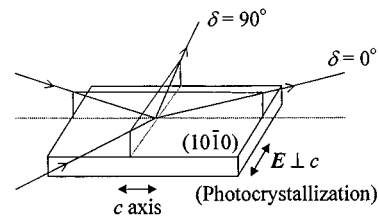


FIG. 3. Reflection of a light beam from a $(10\bar{1}0)$ surface. The light beam is incident at an angle ϕ from the ambient (air) onto a uniaxial crystal with the optic axis c parallel ($\phi = 0^\circ$) and perpendicular to the plane of incidence ($\phi = 90^\circ$).

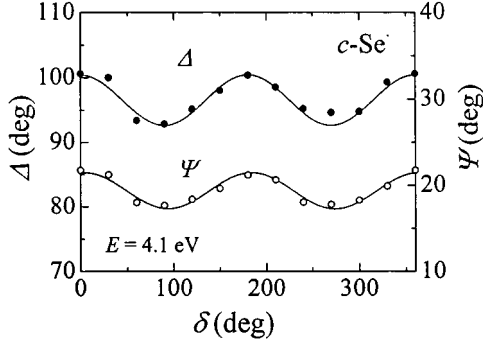


FIG. 4. δ dependence of Δ and ψ for the photocrystallized Se film measured at $E=4.1$ eV.

a -Se, seen in Fig. 2, is typical behavior of amorphous semiconductors. The CP features observed in the thermocrystallized film are due to the appearance of crystal periodicity after annealing. In our measured $\varepsilon(E)$ spectra (Fig. 2), we can find at least three CP's. These are at $E \sim 2.0$, ~ 3.1 , and ~ 3.8 eV.

2. Photocrystallized film

A remarkable difference in the $\varepsilon(E)$ spectra against specimen rotation was observed in the photocrystallized film. This fact implies that the crystallites in the film have a preferred orientation. The XRD data suggested that the film has the $(10\bar{1}0)$ plane as its surface [see Fig. 1(c)]. Note that the $(10\bar{1}0)$ plane thus contains the threefold c axis on its plane. As we will see next, our measured SE data indicated that the c axis is perpendicular to the direction of the polarization of the laser light used for the photocrystallization.

It is very lucky that the film has the $(10\bar{1}0)$ plane as its surface orientation. This allows us to determine a complete set of the optical constants, i.e., those for the ordinary ($\mathbf{E} \perp c$) and extraordinary rays ($\mathbf{E} \parallel c$). If the film had the c plane as its surface orientation, we were unable to determine such a complete set of the optical constants but were able to determine only a set of the optical constants (i.e., only for $\mathbf{E} \perp c$, but not for $\mathbf{E} \parallel c$).¹⁶

Let us assume that the light is incident at an angle ϕ from the ambient onto a uniaxial crystal with the optic axis c parallel and perpendicular to the plane of incidence, as shown in Fig. 3. Fresnel's formulas then allow us to calculate the two complex reflection coefficients r_p and r_s for light polarized parallel and perpendicular to the plane of incidence, respectively. If the c axis is parallel to both the interface and the plane of incidence ($\delta=0^\circ$), Fresnel's reflection coefficients can be simply written as^{17,18}

$$r_p = \frac{\sqrt{\varepsilon_\perp \varepsilon_\parallel} \cos \phi - X_m}{\sqrt{\varepsilon_\perp \varepsilon_\parallel} \cos \phi + X_m}, \quad (1)$$

$$r_s = \frac{\cos \phi - X_m}{\cos \phi + X_m}, \quad (2)$$

with

$$X_m = \sqrt{\varepsilon_\perp - \sin^2 \phi}, \quad (3)$$

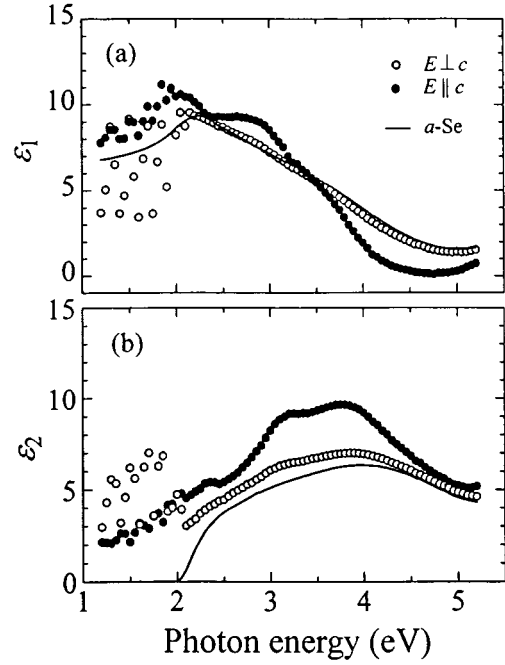


FIG. 5. $\varepsilon(E)$ spectra for the photocrystallized Se film for $\mathbf{E} \perp c$ (open circles) and $\mathbf{E} \parallel c$ (solid circles) measured by SE. For comparison, the spectra taken for the as-deposited a -Se film (Ref. 14) are shown by the solid lines. The oscillations seen in the low photon-energy region ($E < 2$ eV) originate from multiple internal reflections in the film where it is effectively transparent.

where ε_\perp and ε_\parallel represent the complex dielectric constants for the ordinary and extraordinary rays, respectively.

If the c axis is parallel to the interface and perpendicular to the plane of incidence ($\delta=90^\circ$), Fresnel's expression can be given by^{17,18}

$$r_p = \frac{\varepsilon_\perp \cos \phi - X_m}{\varepsilon_\perp \cos \phi + X_m}, \quad (4)$$

$$r_s = \frac{\cos \phi - X_n}{\cos \phi + X_n}, \quad (5)$$

with

$$X_n = \sqrt{\varepsilon_\parallel - \sin^2 \phi}, \quad (6)$$

and X_m is given by Eq. (3).

Ellipsometry yields the complex ratio ρ between Fresnel's reflection coefficients r_p and r_s ,

$$\rho = \frac{r_s}{r_p} = \tan \psi e^{i\Delta}, \quad (7)$$

where Δ and ψ are the ellipsometric variables. At each photon energy $E = \hbar\omega$, the four optical parameters ($\varepsilon_{1\perp}, \varepsilon_{2\perp}, \varepsilon_{1\parallel}, \varepsilon_{2\parallel}$) can be determined from the two pairs of SE measurements [$\rho^{\text{meas}}(\delta=0^\circ, \delta=90^\circ)$] by minimizing the error function $G(\varepsilon_{1\perp}, \varepsilon_{2\perp}, \varepsilon_{1\parallel}, \varepsilon_{2\parallel})$,^{17,18}

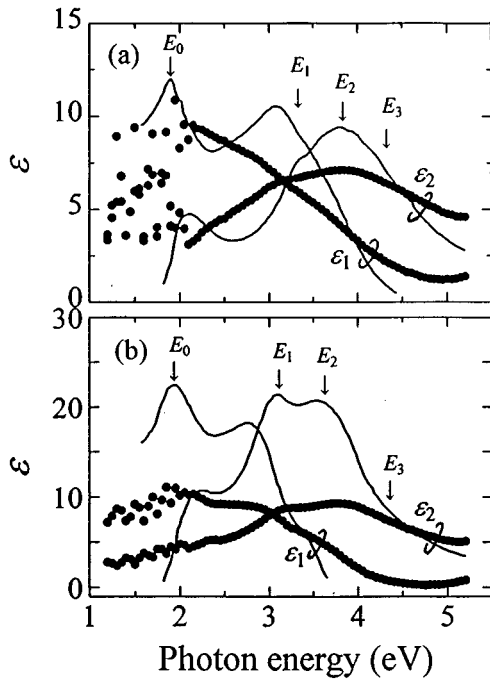


FIG. 6. $\varepsilon(E)$ spectra for (a) $\mathbf{E}\perp c$ and (b) $\mathbf{E}\parallel c$ for the photocrystallized Se film. The solid lines represent the spectra for a bulk, single-crystalline Se obtained from reflectivity measurements by Tutihasi and Chen (Ref. 19). The positions of each CP are marked by the vertical arrows (E_0-E_3).

$$G(\varepsilon_{1\perp}, \varepsilon_{2\perp}, \varepsilon_{1\parallel}, \varepsilon_{2\parallel}) = \sum_{\delta=0^\circ, 90^\circ} \{ [\text{Re}(\rho_\delta^{\text{meas}}) - \text{Re}(\rho_\delta^{\text{calc}})]^2 + [\text{Im}(\rho_\delta^{\text{meas}}) - \text{Im}(\rho_\delta^{\text{calc}})]^2 \}, \quad (8)$$

where ρ^{calc} is the calculated reflection coefficient ratio.

We show in Fig. 4, as an example, the δ dependence of Δ and ψ for the photocrystallized Se film measured at $E = 4.1$ eV. It is easily understood from this figure that Δ exhibits a twofold symmetry with maxima at $\delta = 0^\circ, 180^\circ$, and 360° , corresponding to incident light perpendicular to the c axis ($\mathbf{E}\perp c$), and minima at $\delta = 90^\circ$ and 270° , corresponding to incident light parallel to the c axis ($\mathbf{E}\parallel c$). Plots of ψ versus δ also exhibit a cosine shape with maxima at $\delta = 0^\circ, 180^\circ$, and 360° and minima at $\delta = 90^\circ$ and 270° , indicating that the photocrystallized film is indeed optically uniaxial.

Figure 5 shows the SE $\varepsilon(E)$ spectra for the photocrystallized Se film, together with those for the as-deposited a -Se film (Ref. 14). As clearly seen in the figure, the measured $\varepsilon(E)$ spectra show very strong polarization dependence. As in the thermocrystallized film (Fig. 2), we can find at least three CP's in the measured $\varepsilon(E)$ spectra.

Figure 6 compares the $\varepsilon(E)$ spectra for the photocrystallized film to those for a bulk, single-crystalline Se. The spectra for the bulk, single-crystalline Se were determined from reflectivity measurements by Tutihasi and Chen (Ref. 19). It is understood from Fig. 6 that the strength of each CP in the photocrystallized Se film is weaker than that in the bulk, single-crystalline Se. This is because, as we will see in Sec. III C, the photocrystallized Se film has a considerable degree of the surface roughness. The sum rules used popularly

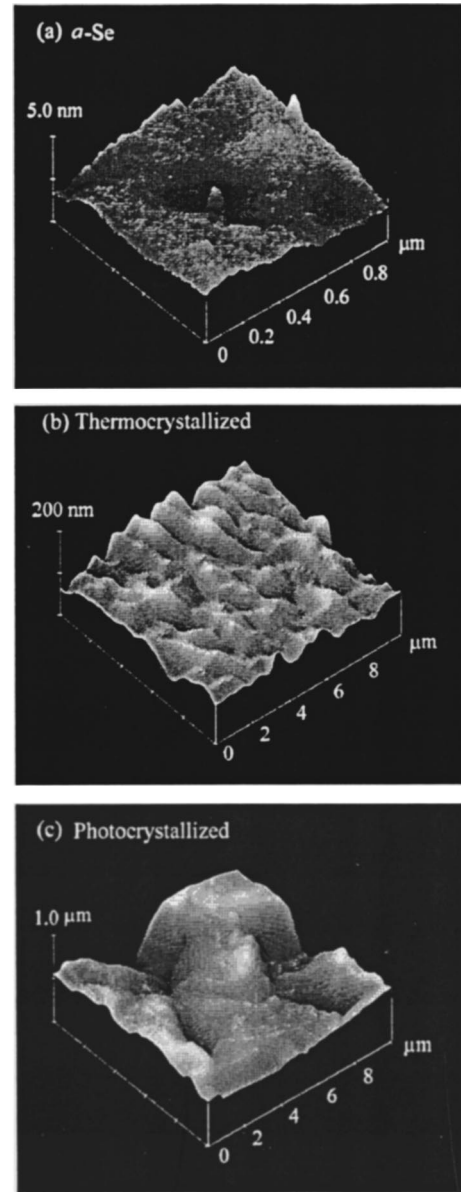


FIG. 7. Large-scale (1×1 or $10 \times 10 \mu\text{m}^2$) AFM images for (a) the as-deposited, (b) thermocrystallized (100°C , 1 h), and (c) photocrystallized Se films.

suppose²⁰ that the presence of voids, or in other words, density deficits in the film medium, reduces the number of effective oscillators per unit volume, resulting in the weak CP-strength feature observed in such roughened film.

C. AFM observation

We used *ex situ* AFM to independently assess surface morphology changes produced by thermal annealing and laser illumination. Figure 7 shows large-scale (1×1 or $10 \times 10 \mu\text{m}^2$) AFM images for (a) the as-deposited a -Se, (b) thermocrystallized, and (c) photocrystallized Se films. The root-mean-square (rms) roughnesses obtained from these figures are, respectively, (a) ~ 0.8 , (b) ~ 13 , and (c) ~ 230 nm. The as-deposited a -Se film is found to have a very flat surface. On the other hand, the thermocrystallized and especially photocrystallized films result in surface roughening.

The surfaces of these films then have a dense conelike [Fig. 7(b)] and a large ridge structure [Fig. 7(c)], respectively.

IV. DISCUSSION

We have studied the structural and optical properties of the photocrystallized Se film deposited on a glass substrate under illumination of a 488.0-nm Ar laser line. The surface orientation of the film is found to be the $(10\bar{1}0)$ plane, and the c axis extended on the surface plane is perpendicular to the direction of the polarization of the illuminating light. These agree with those obtained by Poborchii, Kolobov, and Tanaka⁸ using a He-Ne (632.8 nm) and a Kr laser (647.1 nm). However, these authors obtained as the preliminary data that the use of 514.5-nm Ar green line results in no preference about the c -axis orientation. At this wavelength and also at a 488.0-nm Ar blue line used in this study, absorption will occur very strongly, and consequently, a great number of photoexcited carriers will be produced. It should be noted that the mechanism of photocrystallization is believed to be photoelectronic, i.e., it is associated with the photoexcited electrons and holes.²¹

Roy, Kolobov, and Tanaka⁵ have studied the effects of illumination wavelength on the photocrystallization of a -Se using a Kr and an Ar laser. They observed a preferential growth of the $(10\bar{1}0)$ plane by illuminating a 676.4-nm Kr red line and nonpreferential growth by a 488.0-nm Ar blue line. The 488.0-nm Ar blue line data result is in direct contrast with that obtained by us. The Ar laser power used by Roy, Kolobov, and Tanaka was 120 W/cm^2 , while ours is $\sim 20 \text{ W/cm}^2$. Note that the glass transition temperature in a -Se is very low, $T_g \sim 30^\circ \text{C}$ (Ref. 13). It may, thus, be possible to consider that the disagreement between these two studies is due to whether any laser-heating-induced mechanism was taking place in the photocrystallization process or not.

For c -Se,^{22–25} the first-order allowed optical transitions are \mathbf{k} -conserved direct transitions, and therefore, the interband-transition optical spectrum reflects the joint density of states in specific parts of the Brillouin zone. The prominent joint-density-of-states features were observed experimentally in $\varepsilon(E)$ of c -Se in the 1–15-eV spectral region for both $\mathbf{E} \perp c$ and $\mathbf{E} \parallel c$ polarizations.^{19,26,27} The majority of the theoretical energy-band structure calculations report^{19,23,24} that the lowest direct gap E_0 in c -Se occurs at or close to the corner H of the hexagonally prismatic Brillouin zone. This energy gap determined experimentally is 1.95 eV at 20 K.¹⁹ The direct optical transitions are also expected to occur at the Z , Γ , and K points in the Brillouin zone. The corresponding energy gaps determined experimentally at 20 K are¹⁹ $E_1 \sim 3.3 \text{ eV}$ for $\mathbf{E} \perp c$ and $\sim 3.2 \text{ eV}$ for $\mathbf{E} \parallel c$ (Z); $E_2 \sim 3.5\text{--}3.8 \text{ eV}$ for both $\mathbf{E} \perp c$ and $\mathbf{E} \parallel c$ (Γ); $E_3 \sim 4.3 \text{ eV}$ for $\mathbf{E} \perp c$ and $\sim 4.5 \text{ eV}$ for $\mathbf{E} \parallel c$ (K). The positions of such CP's are marked in Fig. 6 by the vertical arrows.

For a -Se, the $\varepsilon_2(E)$ spectrum showed a broad peak structure (see Fig. 2). Such a spectral feature is typically observed in amorphous semiconductors, and is considered to be due to the breakdown of crystal periodicity in the amorphous state. It has been shown¹⁴ that the $\varepsilon(E)$ data for a -Se can be successfully interpreted by a modified model of Jellison and Modine²⁸ in which the two valence and the two conduction

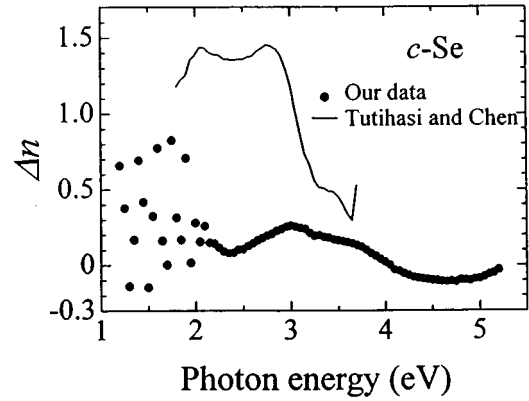


FIG. 8. Birefringence, $\Delta n = n_{\parallel} - n_{\perp}$, for the photocrystallized Se film (solid circles) and that for a bulk, single-crystalline Se (solid line), obtained from Eq. (9) using the $(\varepsilon_1, \varepsilon_2)$ data plotted in Fig. 6.

bands are properly taken into consideration.

SE is very sensitive to surface microroughness. It is possible, in principle, to mathematically remove the effects of surface microroughness from measured $\varepsilon(E)$ data using an effective-medium-approximation (EMA) analysis.^{14,16} However, we found that in the present case this approach is not successful. This is because the mean height and correlation length of the surface irregularities observed on the thermo- and photocrystallized films are comparable or larger than the wavelength of light ($\lambda \sim 0.2\text{--}1 \mu\text{m}$, see Fig. 7). Note that in the EMA analysis, such quantities are required to be less than the wavelength of light.²⁹

Ishida and Tanaka⁴ reported the birefringence $\Delta n = n_{\parallel} - n_{\perp}$ at a wavelength of 632.8 nm in Se films photocrystallized with a linearly polarized 632.8-nm line of a He-Ne laser, where n_{\parallel} and n_{\perp} represent the refractive index for $\mathbf{E} \parallel c$ and $\mathbf{E} \perp c$, respectively. They measured the Δn value as a function of the He-Ne laser power density used for the photocrystallization. The maximum Δn value measured is 0.09 ± 0.04 at 5 W/cm^2 , which is about an order smaller than the natural birefringence in a bulk, single-crystalline Se. We must note, however, that the birefringence of a thin sample will suffer from an internal reflection oscillation at lower photon energies. In fact, as in Figs. 2 and 5, one can easily find in Fig. 8 an oscillation in Δn for energies $E < 2 \text{ eV}$ caused by the internal reflection. Here, the Δn values plotted in Fig. 8 are obtained simply from

$$n(E) = \left(\frac{[\varepsilon_1(E)^2 + \varepsilon_2(E)^2]^{1/2} + \varepsilon_1(E)}{2} \right)^{1/2}, \quad (9)$$

using the $(\varepsilon_1, \varepsilon_2)$ data in Fig. 6. An exact expression for the birefringence in an opaque region is given in Ref. 30.

V. CONCLUSIONS

Structural and optical properties of the photocrystallized Se films were investigated using XRD, SE, and *ex situ* AFM measurement techniques. The photocrystallization of a -Se was achieved by illuminating with a linearly polarized 488.0-nm line of an Ar laser at room temperature. For comparison, properties of the thermocrystallized films at 100°C for 1 h were studied. It was shown that the photocrystallized

film has the $(10\bar{1}0)$ plane as its surface and that the c axis extended on the $(10\bar{1}0)$ surface is perpendicular to the direction of the polarization of the illuminating light. This film geometry enabled us to determine a complete set of the optical constants, i.e., those for the $\mathbf{E}\perp c$ and $\mathbf{E}\parallel c$ polarizations. The thermocrystallized film was found to be characterized by an unoriented polycrystalline structure. The measured SE $\varepsilon(E)$ data showed the weak CP-strength feature in both the photo- and thermocrystallized films. This is because the presence of voids or density deficits in the film medium reduces

the total number of effective oscillators per unit volume, resulting in such a weak CP-strength feature. The surface irregularities produced by the photo- and thermocrystallization were independently assessed by the AFM.

ACKNOWLEDGMENT

This work was supported in part by the Gunma University–Satellite Venture Business Laboratory (GU-SVBL).

-
- ¹J. Dresner and G. B. Stringfellow, *J. Phys. Chem. Solids* **29**, 303 (1968).
- ²V. G. Zhdanov, B. T. Kolomiets, V. M. Lyubin, and V. K. Malinovsky, *Phys. Status Solidi A* **52**, 621 (1979).
- ³K. Tanaka and A. Odajima, *Solid State Commun.* **43**, 961 (1982).
- ⁴K. Ishida and K. Tanaka, *Phys. Rev. B* **56**, 206 (1997).
- ⁵A. Roy, A. V. Kolobov, and K. Tanaka, *J. Appl. Phys.* **83**, 4951 (1998).
- ⁶A. V. Kolobov, H. Oyanagi, K. Tanaka, and K. Tanaka, *Phys. Rev. B* **55**, 726 (1997).
- ⁷A. Roy, A. V. Kolobov, H. Oyanagi, and K. Tanaka, *Philos. Mag. B* **78**, 87 (1998).
- ⁸V. V. Poborchii, A. V. Kolobov, and K. Tanaka, *Appl. Phys. Lett.* **72**, 1167 (1998).
- ⁹K. Tanaka, K. Ishida, and N. Yoshida, *Phys. Rev. B* **54**, 9190 (1996).
- ¹⁰V. Lyubin, M. Klebanov, M. Mitkova, and T. Petkova, *Appl. Phys. Lett.* **71**, 2118 (1997).
- ¹¹V. K. Tikhomirov, P. Hertogen, C. Glorieux, and G. J. Adriaenssens, *Phys. Status Solidi A* **162**, R1 (1997).
- ¹²D. E. Aspnes, in *Handbook of Optical Constants of Solids*, edited by E. D. Palik (Academic, Orlando, 1985), p. 89.
- ¹³Z. U. Borisova, *Glassy Semiconductors* (Plenum, New York, 1981).
- ¹⁴T. Innami, T. Miyazaki, and S. Adachi, *J. Appl. Phys.* **86**, 1382 (1999).
- ¹⁵G. Harbeke, in *Optical Properties of Solids*, edited by F. Abeles (North-Holland, Amsterdam, 1972), p. 21.
- ¹⁶See, for example, T. Kawashima, H. Yoshikawa, S. Adachi, S. Fuke, and K. Ohtsuka, *J. Appl. Phys.* **82**, 3528 (1997).
- ¹⁷S. Logothetidis, M. Cardona, P. Lautenschlager, and M. Garriga, *Phys. Rev. B* **34**, 2458 (1986).
- ¹⁸S. Ninomiya and S. Adachi, *J. Appl. Phys.* **78**, 4681 (1995).
- ¹⁹S. Tutihasi and I. Chen, *Phys. Rev.* **158**, 623 (1967).
- ²⁰S. Adachi and T. Miyazaki, *Phys. Rev. B* **51**, 14 317 (1995).
- ²¹See Ref. 4, and references therein.
- ²²D. J. Olechna and R. S. Knox, *Phys. Rev.* **140**, A986 (1965).
- ²³J. Treusch and R. Sandrock, *Phys. Status Solidi* **16**, 487 (1966).
- ²⁴R. Sandrock, *Phys. Rev.* **169**, 642 (1968).
- ²⁵K. Maschke and P. Thomas, *Phys. Status Solidi* **41**, 743 (1970).
- ²⁶A. G. Leiga, *J. Opt. Soc. Am.* **58**, 880 (1968).
- ²⁷P. Bammes, R. Klucker, E. E. Koch, and T. Tuomi, *Phys. Status Solidi B* **49**, 561 (1972).
- ²⁸G. E. Jellison, Jr. and F. A. Modine, *Appl. Phys. Lett.* **69**, 371 (1996); **69**, 2137(E) (1996).
- ²⁹R. M. A. Azzam and N. M. Bashara, *Ellipsometry and Polarized Light* (North-Holland, Amsterdam, 1977).
- ³⁰S. Adachi and C. Hamaguchi, *Phys. Rev. B* **21**, 1701 (1980).